# A New Strategy to Uncover Fragile X Proteomic Biomarkers Using the Nascent Proteome of Peripheral Blood Mononuclear Cells (PBMCs)

**Olivier Dionne** ( olivier.dionne@usherbrooke.ca )
Sherbrooke University https://orcid.org/0000-0002-0531-9761
**François Corbin**
Sherbrooke University Hospital: Centre integre universitaire de sante et de services sociaux de l'Estrie Centre hospitalier universitaire de Sherbrooke du Quebec

**Research**

**Keywords:** Fragile X syndrome, biomarkers, proteomics, nascent proteome, BONCAT, label-free mass spectrometry, PBMCs, translational medicine

**DOI:** https://doi.org/10.21203/rs.3.rs-146075/v1

# Abstract

**Background:** Fragile X syndrome (FXS) is the most prevalent inherited cause of intellectual disabilities and autism spectrum disorders. FXS result from the loss of expression of the FMRP protein, an RNA binding protein that regulate the expression of key synaptic effectors. FXS is also characterized by a wide array of behavioral, cognitive and metabolic impairments. The severity and penetrance of those comorbidities are extremely variable, meaning that a considerable phenotypic heterogeneity is found among fragile X individuals. Unfortunately, clinicians currently have no tools at their disposal to assay patient's prognosis upon diagnosis. Since the absence of FMRP was repeatedly associated with an aberrant translational metabolism, we decided to study the nascent proteome in order to screen for potential proteomic biomarkers of FXS.

**Method:** We used a BONCAT (Bioothogonal Non-canonical Amino Acids Tagging) method coupled to label-free mass spectrometry to purify and quantify nascent proteins of peripheral blood mononuclear cells from 7 fragile X male patients that do not express FMRP and 7 age-matched controls. Candidate biomarkers were confirmed by Western blot.

**Results:** The proteomic analysis identified several proteins which were either up or downregulated in absence of FMRP in FXS individuals as compared to controls. Eleven of those proteins were considered as potential biomarkers, from which 5 were further validated by Western blot. The gene ontology enrichment analysis highlighted molecular pathway that may contribute to FXS physiopathology.

**Conclusions:** Our results showed that the nascent proteome is well suited for the discovery of FXS biomarkers. In fact, taking advantage of a key alteration in FXS physiopathology led us to successfully identified 11 potential biomarkers.


# Background

Fragile X syndrome (FXS) is a X-linked neurodevelopmental disorder which represent the most prevalent inherited cause of intellectual disabilities (ID) and autism spectrum disorders (ASD). Several other comorbidities are also associated with FXS, including behavioural issues such as anxiety, aggressivity and hyperactivity as well as physical and metabolic anomalies. The penetrance of those problems is highly variable, resulting in a large phenotypical heterogeneity among individuals with Fragile X (FX)[1–3]. FXS typically originate from the expansion of CGG trinucleotide repeats found in the 5' UTR of the *FMR1* gene. The full mutation (n > 200 CGG) is associated with the epigenetic silencing of *FMR1*, and consequently, with the loss of expression of the fragile X mental retardation protein (FMRP)[4,5].

FMRP remains the most valuable biomarker for FXS, since it can be used to identify fragile X individuals and to predict to some degree their cognitive functions [6,7]. Other biochemicals biomarkers have also been proposed [8]. From those, only a handful have actually been tested in a clinical context [9–13]. In fact, clinicians currently have no prognostic tools at their disposal, meaning that the announcement of a FX diagnosis is accompanied by a great deal of uncertainty regarding the severity of the comorbidities

presented by the affected individual. Those facts clearly illustrate one of the actual shortcomings in the management of individuals with FXS and consequently, the need for the discovery of new biomarkers to assess patient's prognosis upon diagnosis.

The discovery of biomarkers using shotgun proteomic approaches faces two major limitations. First, the dynamic expression range of proteins within the proteome makes identification and quantification of low abundance proteins challenging, especially in data-dependent acquisition methods [14]. This fact becomes even more important when considering that weakly expressed proteins are usually critical for the characterisation of physiopathological mechanisms underlying complex pathologies, such as FXS. Secondly, differentially expression analysis of large proteome dataset highlights, most of the times, a plethora of statistically significant dysregulated proteins between samples. However, not all those findings bear significance from a biological standpoint. It is therefore crucial to use an approach that promotes the identification of proteins that are both dysregulated and biologically relevant. Different workflow can be utilized to achieve such outcomes. One of the most straightforward and widely used method consists of the purification of a specific sub-proteome, either by sub-cellular compartments fractionation or by affinity chromatography. Such approaches ultimately produce proteomic samples that are both smaller, which enhance coverage of the proteome, and enriched in biologically relevant proteins [15]. Targeting the sub-proteome that best depicts the diseases-induced defects therefore constitutes the foundation of an efficient screening strategy.

FMRP is a multifunctional RNA binding protein which principally act as a translational regulator, either as a repressor or enhancer[16,17]. Many mRNAs targeted by FMRP play a key role in neurodevelopment and synaptic transmission [18]. In fact, several alterations found in FXS, including the elevated numbers of immature dendritic spines and improper synaptic plasticity, seem related to the absence of FMRP's translational control [19,20] .This prompted us to use the nascent proteome, defined as proteins synthesized in a defined timeframe, for the screening of proteomic biomarkers. We hypothesize that this sub-proteome will help us to overcome problems typically encountered when performing shotgun proteomic experiments for biomarkers discovery. Indeed, we postulate that the nascent proteome, due to the translational defects encountered in FXS, will provide a proteomic signature that is well-suited for such task. Furthermore, peripheral blood mononuclear cells (PBMCs) constitute a non-invasive model which transcriptome is known to moderately correlate with that of neuronal tissues [21] and that can be repeatedly collected, making it ideal for our purpose

In the present report, we used a BONCAT (Bioorthogonal Noncanonical Amino Acid Tagging) method coupled to labeled free mass spectrometry-based proteomic to purify and quantify nascent proteins produced by PBMCs. With this experimental approach, we compared the nascent proteomes of 7 FXS males and 7 age and sex-matched controls and successfully identified differentially expressed proteins that represents potent biomarker candidates for FXS. To our knowledge, this report also constitutes the first proteomic screening for the discovery of biomarkers in native human samples of FX individuals.

# Methods

## Reagents and antibodies

Acid citric dextrose (ACD) tubes were from BD Vacutainer. Ficoll-Paque was purchased from GE Healthcare. Azidohomoalanine (AHA), bicinchonic acid assay kit, Click-it protein reaction kit, biotin alkyne probe, dithiothreitol (DTT), Triton-X100m, C18 tips, goat polyclonal anti-biotin and goat anti-rabbit Alexa FluorVR 680 IgG antibodies were from ThermoFisher. RPMI 1640 $Met^-$, P8340 protease inhibitor cocktail, magnetics streptavidin beads, ammonium bicarbonate (ABC), iodoacetamide (IAA), formic acid (FA), mouse monoclonal anti-actin (clone AC-15), Donkey anti-goat IgG, and goat anti-rabbit IgG HRP-conjugated antibodies were bought from MilliporeSigma. Trypsin/lys-C and the enhanced chemiluminescence kit (ECL) were from Promega and PerkinElmer respectively. Rabbit monoclonal anti-ILK (EP1593Y), rabbit monoclonal anti-ANXA2 (ERP13052B) and mouse monoclonal anti-FERMT3 (3D6) were from Abcam. Mouse monoclonal anti-ATP2A3 (PL/IM430) was from Santa Cruz Biotechnology. Recombinant chicken anti-VCL antibody was from Immune Biosolutions. Goat anti-mouse IgG HRP-conjugated was from Jackson IR. Goat anti-mouse IRDyeVR 800CW IgG was from LI-COR Biosciences.

## Study population and ethics

The study population included 7 FX patients and 7 healthy controls. Participants were all males and were matched for age. The recruitment was performed through the Fragile X Clinic, at the *CIUSSS de l'Estrie-CHUS* (Sherbrooke, Québec, Canada). Informed written consent was obtained from healthy controls and from a caregiver for FXS participants in accordance with requirements of the Ethics Review Board of the *CIUSSS de l'Estrie-CHUS*. All participants had blood draw in the morning to decrease potential diurnal variation.

## PBMCs isolation

PBMCs isolation was carried out using Ficoll-Paque following the manufacturer instructions with some minor modifications. Briefly, blood sample were collected by venipuncture into 8 mL ACD tubes and centrifuged at 300g for 10 minutes to allow plasma collection. A volume of PBS, equal to the volume of plasma collected, was then added to each tube and resulting blood samples were place onto a layer of Ficoll-Paque (blood/Ficoll-Paque ratio of 4:3). Afterwards, samples were centrifuged at 500g for 30 minutes. PBMCs were subsequently collected, washed two times with PBS and counted on a flow cytometer (DXH-9000 hematology analyzer, Beckman Coulter®).

## AHA labeling

We used the metabolic labeling of the nascent proteins by BONCAT to isolate the nascent proteins from the whole proteome. In this approach, newly synthesis proteins are labelled with azidohomoalanine, an azide bearing methionine analogue, before being conjugated to a biotin alkyne probe. Nascent proteins are subsequently purified by a streptavidin pull-down and analyzed by mass spectrometry [22].

Freshly extracted PBMCs were first resuspended into warm (37°C) RPMI 1640 $Met^-$ (supplemented with 2 mM L-Glutamine) and incubated for 30 minutes at 37°C under gentle agitation to deplete the intracellular reserve of methionine. PBMCs were then diluted to a concentration of 3 million cells/mL and labeled with 100 µM AHA for two hours. Cells were pelleted and stored at -80°C after labelling. The optimised labeling conditions as well as the specificity of the AHA labeling and subsequent Click reaction toward nascent proteins were determined by Western blot using a specific anti-biotin antibody (Figure 1).

### PBMCs protein extract

PBMCs were lysed in ice-cold 50 mM Tris pH 8.0, 1% NaDoc, 1% P8340 protease inhibitor cocktail and 250 U/mL Benzonase nuclease. After 15 minutes on ice, cells were homogenised with a 28G needle and proteins were pelleted for 25 minutes at 20 000g (4°C). Protein quantification in the supernatant was determined by bicinchonic acid assay.

### Isolation of nascent proteins and preparation for MS analysis

Two experimental groups were formed (Control and FX) by pooling an equal amount of protein from each participant. The conjugation of the biotin probe was performed on 150 µg of pooled proteins using the Click-it protein reaction kit, following the manufacturer instructions and using a biotin alkyne probe. Nascent biotinylated proteins were purified by an overnight incubation with magnetics streptavidin beads at 4°C. The beads were washed 4 times with PBS containing 0.1% Triton X-100 and 5 times with a 20 mM pH 8.0 ABC (ammonium bicarbonate) buffer. Cysteines reduction was realized by incubating the beads with 10 mM DTT at 60°C for 30 minutes and subsequent alkylation with 15 mM iodoacetamide for 30 minutes at room temperature in the dark. Proteins digestion into peptide was performed overnight at 37°C with 1 µg of trypsin/lys-C. The digestion was stopped by adding formic acid to a final concentration of 1%. The supernatant was transferred to a clean tube and the beads were washed two times with 60% acetonitrile in 0.1% formic acid. All supernatants were combined and evaporated. The peptide samples were reconstituted in 0.1% trifluoroacetic acid, desalted with a C18 tip and dried. Nascent proteins were suspended in 1% formic acid and kept at -20°C. Four technical replicates were made for each experimental group, and each replicate was injected twice into the mass spectrometer (intra-assay replicate).

### Preparation of PBMCs total proteome for MS analysis

The same experimental groups used in the previous section were also used for the preparation of the total proteome. Briefly, 5 µg of pooled protein extracts were solubilized with 8M urea in 10 mM HEPES pH 8.0 (protein/urea ratio (p/v) of 1:1). Reduction of proteins was performed with 10 mM DTT at 60°C for 30 minutes and alkylation with 15 mM IAA at room temperature in the dark for 30 minutes. Urea concentration was lowered below 1M by adding 50 mM pH 8.0 ABC buffer. Proteins digestion into peptide was performed overnight at 37°C with 0.25 µg (ratio trypsin/protein of 1:20) of trypsin/lys-C and stopped by adding 1% formic acid. Peptide samples were evaporated, desalted with a C18 tip and evaporated. The total proteome was suspended in 1% formic acid and kept at -20°C. Four technical replicates were made

for each experimental group, and each replicate was injected twice into the mass spectrometer (intra-assay replicate).

### LC-MS/MS analysis

Peptide were injected into an HPLC (nanoElute, Bruker Daltonics) and loaded onto a trap column with a constant flow of 4 µl/min (Acclaim PepMap100 C18 column, 0.3 mm id x 5 mm, Dionex Corporation) and eluted onto an analytical C18 Column (1.9 µm beads size, 75 µm x 25 cm, PepSep). Peptides were eluted over a 2-hour gradient of acetonitrile (5-37%) in 0.1% formic acid at 400 nL/min while being injected into a TimsTOF Pro Mass Spectrometer equipped with a Captive Spray nano electrospray source (Bruker Daltonics). Data were acquired using data-dependent auto-MS/MS with a 100-1700 m/z mass range, with PASEF enabled with a number of PASEF scans set at 10 (1.27 seconds duty cycle) and a dynamic exclusion of 0.4 minute, m/z dependent isolation window and collision energy of 42.0 eV. The target intensity was set to 20,000, with an intensity threshold of 2,500.

### Mass spectrometry data analysis

Proteins identification from the raw data was accomplish with the MaxQuant software[23] (version 1.6.10.0). Peaks list was searched against the Uniprot human database (09/2019). Trypsin was set as digestion enzyme with specificity for arginine and lysine (but not before proline). A maximum of two miss cleavages was tolerated. Oxidation of methionine and acetylation of proteins N-terminus were set as variable modifications, while carbamidomethylation of cysteine was set as a fixed modification. Carbamylation of lysine was set as variable modification only for the analysis of the total proteome. False discovery rate of peptide (minimum of 7 amino acids) and proteins was set to 0.05 using a reverse database. The mass tolerance was set to 7 ppm for precursor ions and 20 ppm for fragment ions. The MaxQuant label free quantification (LFQ) was used, with a minimum ratio count of two, for accurate intensity based quantification of proteins between samples[24].

### Proteomic data processing

Processing of proteomics data was carried out with the Perseus software[25] (version 1.6.7.0.). Proteins identified as "potential contaminant", "only identified by site" or "reverse" by MaxQuant were excluded. Data was normalized (average intensities of each sample equal within each group) before further analyzes. Proteins only identified in at least 50% of the samples from each group with a minimum of 1 unique peptide and 2 total peptides were kept. The statistical significance of proteins expression between the two groups was evaluated by a two-tailed student T-test, carried out in the Perseus software ($p < 0.05$ for the nascent proteome; $p < 0.01$ after correction with a permutation-based FDR, for the total proteome analysis). We choose to be more stringent for the differential expression analysis carried out for the total proteome to lower the numbers of statistical hits. The corresponding volcano plots were drawn using the ggplot2 package in R.

For the nascent proteome analysis, a "negative control" was produced to eliminate contaminating and endogenous biotinylated proteins. To achieve this, an unlabeled protein extract from a control PBMCs was subjected to all the steps of the workflow describe above (Click reaction, streptavidin pulldown, on beads proteins preparation for MS analysis etc.). Proteins identified with a fold change (experimental sample/negative control) superior to 1.1 where kept for further analysis. Proteins that do not fulfill this criterion where excluded.

### Bioinformatic analysis

Functional annotation enrichment analyses were carried out with the Panther classification system ( www.pantherdb.org ) using the Gene Ontology, Panther protein class and REACTOME pathways annotations sets [26–28]. Protein-protein interaction network (PPI) analysis were obtained from the web-based LENS tool (Lens for Enrichment and Network Studies of Proteins) at the website: http://severus.dbmi.pitt.edu/LENS [29].

### Western Blots

Optimal AHA labeling conditions and specificity towards newly synthetized proteins were confirmed by an anti-biotin Western blot (Figure 1). Briefly, 10 µg of proteins sample were resolved on a 10% SDS-PAGE, transferred onto a nitrocellulose membrane, block with 5% non-fat dry milk and incubated with the following antibodies: anti-biotin (1:1000) and anti-actin (1:5000). Blots were revelated using an enhanced chemiluminescence (ECL) kit and imaged with ChemiDoc (Bio-Rad).

Western blots were also used to validate 5 proteins found dysregulated in fragile X PBMCs by the proteomic screening (ILK, ATP2A3, ANXA2, FERMT3 and VCL). Briefly, 15 µg of proteins from each participant were resolved on a 9% (ILK, ATP2A3 and VCL) or a 12% (ANXA2 and FERMT3) SDS-PAGE, transferred onto a nitrocellulose membrane, block with 5% non-fat dry milk and incubated with the following antibodies: anti-ILK (1:2000), anti-ANXA2 (1:2000), anti-ATP2A3 (1:250), anti-FERMT3 (1:2000), anti-VCL (1:1000) and anti-actin (1:5000).Anti-goat IgG (1:10 000), anti-mouse IgG (1:10 000) and anti-rabbit IgG (1:10 000) HRP-conjugated secondary antibodies were used for ECL revelation, while anti-mouse IRDyeVR 800CW IgG (1:10 000) and anti-rabbit Alexa FluorVR 680 IgG (1:10 000) were used for fluorescence-based immunostaining. All immunoblots were analysed with the Image-J software (NIH). Immunoblots were revelated either by ECL (imaged with ChemiDoc, BioRad) or by fluorescence (imaged with the Odyssey Infrared Imaging System, LI-COR Biosciences).

### Statistical analyses

Fisher exact tests were used with R studio to perform Gene Ontology enrichment analysis. A p-value inferior to 0.05 (corrected with a permutation-based FDR) was considered significative. For the Western blot analysis, statistically significant difference was determined by a two-tailed student t-test calculated in GraphPad Prism (version 8.3.0). A p-value inferior to 0.05 was considered significative.

# Results

## Population characteristics

The study population included 7 fully mutated males with fragile X (mean age of 28.7 ± 9.0) and 7 healthy males (mean age of 27.7 ± 8.1). Individuals characteristics of each participants, including age, medication and fragile X diagnostic are listed in Table 1.

Table 1

Individuals characteristics of each participant

| ID | Age | Sex | Medication | Fragile X | diagnostic |
|---|---|---|---|---|---|
| Fragile X cohort | | | | | |
| X1 | 25 | Male | | Full mutation | |
| X2 | 40 | Male | Levothyroxine, antispychotic (Olanzapine) | Full mutation | |
| X3 | 17 | Male | | Full mutation | |
| X4 | 29 | Male | | Full mutation | |
| X5 | 43 | Male | | Full mutation | |
| X6 | 30 | Male | Anti-diabetic (Metformin) | Full mutation | |
| X7 | 25 | Male | | Full mutation | |
| Control cohort | | | | | |
| C1 | 24 | Male | | NA | |
| C2 | 23 | Male | | NA | |
| C3 | 41 | Male | Antiandrogen (Finasteride) | NA | |
| C4 | 26 | Male | | NA | |
| C5 | 18 | Male | | NA | |
| C6 | 34 | Male | Levothyroxine | NA | |
| C7 | 35 | Male | | NA | |

## The nascent proteome harboured distinct characteristics suited for the discovery of FXS biomarkers

As shown in Figure 2A, the nascent proteome is far less complex then its total counterpart. Contrary to our assumption, this distinct feature of the nascent proteome did not allow for a better proteome coverage. Indeed, only 7 of the 109 proteins identified in the nascent proteome were not identify among the 1770 proteins within the total proteome. On the other hand, the nascent proteome displays an enrichment for proteins whose functions are well suited for the characterisation of the translation defects caused by FMRP's absence. Indeed, the nascent proteins identified are involved in nucleic acid, nucleoside and protein binding as well as in cellular component organisation or biogenesis (Figure 2B, C and D). Moreover, 5 of the 7 proteins identified only in the nascent proteome are found dysregulated in fragile X PBMCs (Table 2). Taken together, those results support our hypothesis that the isolation of nascent proteins will promotes the identification of dysregulated proteins between FX patients and control individuals that are also relevant from a biological standpoint.

### Differentially expressed proteins are found in PBMCs nascent and total proteome

Analysis of the total proteome successfully identified 1770 distinct proteins. More precisely, 1752 and 1768 were identified in fragile X and control individuals respectively (Additional file 1). From those proteins, 200 where found to be dysregulated in FXS samples (Figure 3A). Indeed, 135 where found to be upregulated while 65 where found downregulated (Additional file 2). On the other hand, the BONCAT approach made it possible to identify a total of 109 nascent proteins, 105 from the FXS patients and 106 from control samples (Additional file 3). Thirty nascent proteins where found dysregulated in FX PBMCS (Figure 3B), from which 17 where upregulated and 13 downregulated (Table 2). Noteworthy, 11 dysregulated proteins were identified using both approaches (AHNAK, ATP2A3, PDIA3, PF4, TLN1, FERMT3, HIST1H4A, ILK, MPO, ANXA2 and VCL). Those proteins, which will be refer has strong candidates, represent potential biomarkers of FXS. The trend of expression of those proteins (except for ATP2A3, PDIA3, PF4 and ANXA2) where found to be consistent between the two proteomes (Figure 3C and Table 2).

Table 2

Differentially expressed proteins in the fragile X nascent proteome. 30 proteins are found differentially expressed ($p < 0.05$) in the nascent proteome of the fragile X group. From those proteins, 11 are also found dysregulated in the total proteome ($q < 0.01$) of the fragile X group and 5 where only detected in the nascent proteome.

| Gene names | Protein names | Fold change nascent proteome | p-value nascent proteome | Fold change total proteome | q-value total proteome |
|---|---|---|---|---|---|
| AHNAK | Neuroblast differentiation-associated protein AHNAK | 0.087 | < 0.0001 | 0.704 | < 0.0001 |
| ATP2A3 | Sarcoplasmic/endoplasmic reticulum calcium ATPase 3 | 0.193 | 0.048 | 1.168 | < 0.0001 |
| PDIA3 | Protein disulfide-isomerase A3 | 0.288 | 0.003 | 1.121 | < 0.0001 |
| PF4 | Platelet factor 4 | Detected only in the control group | 0.037 | 1.252 | < 0.0001 |
| TLN1 | Talin-1 | 1.497 | 0.024 | 1.369 | < 0.0001 |
| FERMT3 | Fermitin family homolog 3 | 1.412 | 0.001 | 1.202 | < 0.0001 |
| HIST1H4A | Histone H4 | 2.861 | < 0.0001 | 1.188 | < 0.0001 |
| ILK | Integrin-linked protein kinase | 1.684 | 0.034 | 1.342 | < 0.0001 |
| MPO | Myeloperoxidase | 5.157 | 0.001 | 1.115 | < 0.0001 |
| ANXA2 | Annexin A2 | 2.735 | 0.037 | 0.818 | < 0.0001 |
| VCL | Vinculin | 3.013 | 0.034 | 1.330 | < 0.0001 |
| SPP2 | Secreted phosphoprotein 24 | 0.131 | 0.045 | Not detected | NA |
| HIST1H2AC; HIST3H2A | Histone H2A type 1-C; Histone H2A type 3; Histone H2A type 1-B/E | 2.361 | < 0.0001 | Not detected | NA |
| PRPF40A | Pre-mRNA-processing factor 40 homolog A | 3.052 | < 0.0001 | Not detected | NA |
| PRPF38B | Pre-mRNA-splicing factor 38B | 19.741 | < 0.0001 | Not detected | NA |
| AP3D1 | AP-3 complex subunit delta-1 | Detected only in the fragile X group | 0.028 | Not detected | NA |
| GNAI2 | Guanine nucleotide-binding protein G(i) subunit alpha-2 | 0.487 | 0.016 | 0.993 | ns |

| | | | | | |
|---|---|---|---|---|---|
| NCL | Nucleolin | 0.402 | 0.035 | 1.045 | ns |
| DEK | Protein DEK | 0.414 | 0.015 | 0.853 | ns |
| H1FX | Histone H1x | 0.436 | 0.017 | 1.186 | ns |
| RAB1B; RAB1C | Ras-related protein Rab-1B; Putative Ras-related protein Rab-1C | Detected only in the control group | 0.007 | 1.161 | ns |
| SNRPD3 | Small nuclear ribonucleoprotein Sm D3 | Detected only in the control group | 0.014 | 1.009 | ns |
| SNRPE | Small nuclear ribonucleoprotein E | 0.147 | 0.008 | 0.833 | ns |
| RPL30 | 60S ribosomal protein L30 | Detected only in the control group | 0.035 | 0.828 | ns |
| RPL7 | 60S ribosomal protein L7 | 2.799 | 0.022 | 0.972 | ns |
| H2AFY | Core histone macro-H2A.1 | 2.257 | 0.010 | 1.007 | ns |
| NOP58 | Nucleolar protein 58 | 2.680 | 0.015 | 1.049 | ns |
| RPS18 | 40S ribosomal protein S18 | 3.767 | 0.024 | 0.955 | ns |
| PCBP1 | Poly(rC)-binding protein 1 | Detected only in the fragile X group | 0.046 | 1.330 | ns |
| TOP1 | DNA topoisomerase 1 | Detected only in the fragile X group | 0.019 | 0.547 | ns |

### Bioinformatic analysis of the differentially expressed proteins

Functional annotation enrichment analysis of the differentially expressed proteins found in the total proteome of FX PBMCs was carried out with PANTHER. We used all the 1770 proteins identified in the total proteome as reference. Results showed that dysregulated proteins are involved in cellular adhesion, platelets aggregation and degranulation, MAPK2 and MAPK activation and in signaling pathways related to the MAPK and integrins (Figure 4).

A PPI network of the 11 proteins found differentially expressed in FX nascent and total proteome (Table 2) is illustrated in Figure 5A. This network shows that these proteins have commons interaction partners, strongly suggesting a potential interaction between them and their involvement in the same biological pathways. A second PPI network was generated using the same 11 proteins set as candidates and with the FMR1 gene set as target. As illustrated in Figure 5B, all proteins were found to be enriched in this

network, showing that the 11 candidates possess common interaction partners with FMRP. This result suggests the implication of those 11 proteins in molecular mechanism in which FMRP is involved, and consequently, the involvement of their dysregulation in the mechanism underlaying FXS physiopathology. It is also noteworthy that two proteins (NCL and PRPF40A) differentially expressed in the nascent proteome are present in the interaction network containing FMRP and the 11 candidate proteins.

All those observations are supported by the statistics associated with the LENS analysis (Additional file 4), in which three values are used to describe the network connectivity. These values include "minimum shortest path length", "average shortest path length" and the number of "disconnected nodes". Those results support the fact that the two networks are well enriched. Indeed, all three values are less important in "candidates" when only the 11 candidates are given has well as in "candidate to target" when compared to the values associated with "candidate to random" and "target to random".

### Validation of candidate proteins by Western Blot

Five of the 11 proteins differentially expressed in both nascent and total proteome (ILK, ATP2A3, ANXA2, FERMT3 and VCL) from pooled samples of FX PBMCs were chosen to be validated by Western blot (Figure 6). The trend of perturbation of ILK, ATP2A3, ANXA2 and VCL measured by Western blot was consistent with that measured by mass spectrometry. Furthermore, the difference measured for ILK ($p = 0.0250$) and ANXA2 (0.0394) were found to be statistically significant.

## Discussion

The discovery of biomarkers using shotgun proteomic workflow recurrently led to the identification of a high number of protein candidates. Most of them might ultimately be irrelevant, meaning that a lot of time and resources are spent on selection and validation of newly identified candidates before using them in a clinical setting. This is particularly true when screening experiments are conducted on human biological samples. Indeed, disease-induced heterogeneity and interindividual variability inherent to the use of such samples both add an extra level of intricacy to this already complex equation. One way to limit those drawbacks involves the elaboration of a comprehensive targeted strategy and a rigorous experimental procedure. Indeed, a careful selection of affected individuals and the use of a subproteome that specifically aims at the biological defects induced by the studied pathology can lead to the identification of a higher yield of valuable biomarkers.

In the current study, we deliberately selected 7 fully mutated FXS males in order to restrain the etiologic heterogeneity within our FX cohort. The inclusion of mosaic or female patients (which both expressed variable level of FMRP) would have greatly increased the variability of our proteomic analysis[6,7]. Furthermore, we chose to study the nascent proteome to screen for proteomic biomarkers, since it is well established that the absence of FMRP leads to the dysregulation of a subsets of proteins. Indeed, as shown by the annotation enrichment analysis (Figure 2 C-D), the proteins identified in the nascent proteome are well adapted to portray the perturbation of the translational metabolism induce by the lack of FMRP. Our strategy successfully identified 30 dysregulated proteins among the nascent proteome of

FX individuals, a subset that approximately represent 28% of all nascent identified proteins (Table 2). For comparison, up to 11% of the proteins identified in the total proteome were shown to be dysregulated. Moreover, the mRNA of 17 of those 30 proteins were shown to be bound by FMRP [30]. Considered as a whole, these results withstand PBMC's nascent proteome as a promising way to identify potential biomarkers for FXS.

It is well known in the proteomic field that different strategies leads inevitably to a different set of biomarkers. Remarkably, more than 35% of proteins found dysregulated in the nascent proteome of FX were also shown to be dysregulated in our total proteome analysis elevating these 11 proteins as strong biomarker candidates (Figure 2A and Table 2). We further validated the dysregulated expression of 5 of those 11 candidates (ILK, ATP2A3, ANXA2, FERMT3 and VCL) by Western blot using the total proteome of PBMCs. Furthermore, as supported to by the PPI network (Figure 5B), many of those 11 proteins can be associated, because of their function and interaction, to the biological process involved in FXS physiopathology.

One of those validated candidates is the ANXA2 protein. The latter inhibits the degradation of LDL-receptors meditated by the Proprotein convertase subtilisin/kexin type 9 (PCSK9). Such function is achievable through the binding of ANXA2 to PCSK9, which can occurred in a both intra and extracellular manners [31–33]. We have previously found a high rate of hypocholesterolemia in the FX population [3]. Furthermore, there was no correlation between the plasma level of PCSK9 and LDL-cholesterol in FX individuals, a phenomenon which is however observed in healthy controls [3,34]. Here we report a dysregulation of ANXA2 expression in FXS which provides new insides of the underlaying mechanism of hypocholesterolemia reported in this population. Further studies are warranted to validate the interaction between FMRP, ANXA2, PCSK9 and cholesterol levels. ANXA2 is also known to interact with S100A10 and AHNAK (another candidate of this study) to form a complex that increase cell surface expression of L-type Voltage gated calcium channels in mouse brain[35]. AHNAK also promotes the activity of the Raf/MEK/ERK signaling cascade, a pathway hyperactivated in the brain of KO mice and in FX patients blood cells [9,36–39]. Interestingly, a recent study has found a dysregulation in the expression of AHNAK in PBMCs of children with idiopathic ASD, suggesting the dysregulation of AHNAK as a shared pathophysiological mechanism of both conditions [40].

Three others validated candidates (FERMT3, ILK and VCL), along with TLN1 (another candidate of this study), are involved in integrin activation and/or subsequent signal transduction[41–43]. Furthermore, the functional annotation enrichment analysis (Figure 4) shown that the proteins dysregulated in FX PBMCs are associated to biological process related to cells adhesion and, consequently, in integrins signalisation and underlaying signaling cascades. Taken together, those observations suggest an alteration of integrin mediated signaling in FXS. Integrins activation leads to a multitude of cellular process which are transduced by many signaling pathways, such as the Raf/MEK/ERK and PI3K/AKT/mTOR cascades[43–48], both of which are known to be upregulated in KO mice and in cells derived form FX individuals[9,36–39,49–51]. Integrins are also involved in many neuronal processes, including neurite outgrowth, synapse formation and synaptic transmission[52–54]. Impairing integrin binding to the extracellular matrix (ECM)

with RGD peptides (a sequence recognise by integrin extracellular domains) reduced synaptic strength by promoting a decrease in post-synaptic AMPA receptors expression[52,53,55–57]. In neuronal tissue, RGD peptides can be released by the enzymatic activity of the metalloproteinase 9 (MMP9) towards the components of the ECM[56]. The overexpression of MMP9 found in the brain of Fmr1 KO mice and in FXS patients[10,58–61] can therefore be associated to the impaired synaptic plasticity observed in animal models of the disorder [62–65]. These observations, along with dysregulation of FERMT3, ILK, TLN1 and VCL in fragile X PBMCs suggest that dysregulation of integrin activity play a role in FXS molecular physiopathology and that peripheral blood cells, such as PBMCs or platelets, are relevant models to address this hypothesis[41,66,67].

The principal limitation of our study consists in the somewhat low number of proteins identified, especially in the nascent proteome. One possible explanation for this drawback reside in the variations regarding turnover rates between different proteins. Some of the most abundant proteins (ex: histones, cytoskeletal. heat shock proteins etc.) presents very high turnover rates [68], which mean that they can hindered the identification of low abundant proteins in the nascent proteome. The two hours timeframe used to label nascent proteins may also have contributed to reduce the number of proteins identified since it favors only proteins with high turnover rate. Despites these potential limitations, the number of nascent proteins identified in PBMCs is similar to the one reported by another study [69]. Our experimental workflow, which consisted in the processing of pooled samples, can also have limited the scope of our analysis by limiting our capacity to individually assess each participant's unique proteome. The quantitative aspect of this study is also limited, as it the case for all label-free based shotgun proteomic experiments. As such, all the candidates identified in this study will have to be extensively validated in a larger population before being confirmed as FX biomarkers.

# Conclusion

We took advantage of the known translational defects caused by the absence of FMRP to identify several promising biomarkers in FXS. Furthermore, our strategy allows for a minimal recruitment of patients, which limited the inter-individual variation within our FX cohorts, a known caveat of human samples. Obviously, further validation of those biomarkers in a larger FX cohort in relation to clinical profile is warranted. Nevertheless, the strategy put forth in the present study clearly indicates the feasibility, even for rarer disease, to uncover strong biomarkers using pathology-driven sub-proteomic strategies with limited human samples.

# List Of Abbreviations

**ABC:** Ammonium bicarbonate

**ACD:** Acid citric dextrose

**AHA:** Azidohomoalanine

**ASD:** Autism spectrum disorders

**BONCAT:** Biorthogonal non-canonical amino acids tagging

**DTT:** Dithiothreitol

**ECL:** Enhance chemiluminescence

**FMRP:** Fragile X mental retardation protein

**FX:** Fragile X

**FXS:** Fragile X syndrome

**HEPES:** (4-(2-hydroxyethyl) -1-piperazineethanesulfonic acid

**IAA:** Iodoacetamide

**ID:** Intellectual disabilities

**NaDoc:** Sodium deoxycholate

**PBMCs:** Peripheral blood mononuclear cells

**PBS:** Phosphate buffer saline

**PPI:** Protein-protein interaction

**RPMI:** Roswell Park Memorial Institute Medium

# Declaration


### Acknowledgements

We warmly thank all participants and their family for their participation in this study. We are grateful to Dr. Artuela Çaku, Pr. Jean-François Lepage and Armita Abolghasemi for critical review of the manuscript.


### Ethics approval and consent to participate

This study was conducted according to the World Medical Association Declaration of Helsinki. Informed written consent was obtained directly from healthy controls or through a caregiver for FXS participants in accordance with requirements of the Ethics Review Board of the *CIUSSS de l'Estrie-CHUS*.

### Consent for publication

Not applicable.

### Availability of data and materials

All data generated or analyzed during this study are included in this article. If any additional information is required, it may be obtained by request from the corresponding author.

### Competing interest

The authors declare that they have no competing interest.


### Funding

This work was supported by the Centre de Recherche du CHUS and the Foundation of the Stars. The funders had no role in study design, data collection and analysis, decision to publish or preparation of the manuscript. OD holds a Frederick Banting and Charles Best Canada Graduate Scholarship Master Award from the Canadian Institutes of Health Research (CIHR) and a Master Scholarship from the Fonds de Recherche du Québec – Santé (FRQS).


### Authors contribution

FC and OD designed the study. FC requested funding, supervised the study, recruited fragile X individuals and revised the manuscript. OD performed the experiments, data analysis, wrote the original draft and recruited control individuals. All authors read and approved the final manuscript.

# References


1. Ciaccio C, Fontana L, Milani D, Tabano S, Miozzo M, Esposito S. Fragile X syndrome: a review of clinical and molecular diagnoses. Ital J Pediatr [Internet]. 2017 [cited 2019 Nov 19];43. Available from: https://www.ncbi.nlm.nih.gov/pmc/articles/PMC5395755/
2. Kidd SA, Lachiewicz A, Barbouth D, Blitz RK, Delahunty C, McBrien D, et al. Fragile X Syndrome: A Review of Associated Medical Problems. Pediatrics. 2014;134:995–1005.
3. Çaku A, Seidah NG, Lortie A, Gagné N, Perron P, Dubé J, et al. New insights of altered lipid profile in Fragile X Syndrome. Bardoni B, editor. PLOS ONE. 2017;12:e0174301.
4. Pieretti M, Zhang F, Fu Y-H, Warren ST, Oostra BA, Caskey CT, et al. Absence of expression of the FMR-1 gene in fragile X syndrome. Cell. 1991;66:817–22.
5. Verkerk AJMH, Pieretti M, Sutcliffe JS, Fu Y-H, Kuhl DPA, Pizzuti A, et al. Identification of a gene (FMR-1) containing a CGG repeat coincident with a breakpoint cluster region exhibiting length variation in fragile X syndrome. Cell. 1991;65:905–14.
6. Lessard M, Chouiali A, Drouin R, Sébire G, Corbin F. Quantitative measurement of FMRP in blood platelets as a new screening test for fragile X syndrome. Clinical Genetics. 2012;82:472–7.
7. Kim K, Hessl D, Randol JL, Espinal GM, Schneider A, Protic D, et al. Association between IQ and FMR1 protein (FMRP) across the spectrum of CGG repeat expansions. PLoS ONE. 2019;14:e0226811.

8. Zafarullah, Tassone. Molecular Biomarkers in Fragile X Syndrome. Brain Sciences. 2019;9:96.
9. Pellerin D, Çaku A, Fradet M, Bouvier P, Dubé J, Corbin F. Lovastatin corrects ERK pathway hyperactivation in fragile X syndrome: potential of platelet's signaling cascades as new outcome measures in clinical trials. Biomarkers. 2016;21:497–508.
10. Dziembowska M, Pretto DI, Janusz A, Kaczmarek L, Leigh MJ, Gabriel N, et al. High MMP-9 activity levels in fragile X syndrome are lowered by minocycline. American Journal of Medical Genetics Part A. 2013;161:1897–903.
11. Erickson CA, Wink LK, Ray B, Early MC, Stiegelmeyer E, Mathieu-Frasier L, et al. Impact of acamprosate on behavior and brain-derived neurotrophic factor: an open-label study in youth with fragile X syndrome. Psychopharmacology. 2013;228:75–84.
12. Erickson CA, Ray B, Maloney B, Wink LK, Bowers K, Schaefer TL, et al. Impact of Acamprosate on Plasma Amyloid-β Precursor Protein in Youth: A Pilot Analysis in Fragile X Syndrome-Associated and Idiopathic Autism Spectrum Disorder Suggests a Pharmacodynamic Protein Marker. J Psychiatr Res. 2014;59:220–8.
13. AlOlaby RR, Sweha SR, Silva M, Durbin-Johnson B, Yrigollen CM, Pretto D, et al. Molecular biomarkers predictive of sertraline treatment response in young children with fragile X syndrome. Brain Dev. 2017;39:483–92.
14. Ludwig C, Gillet L, Rosenberger G, Amon S, Collins BC, Aebersold R. Data-independent acquisition-based SWATH-MS for quantitative proteomics: a tutorial. Mol Syst Biol. 2018;14:e8126.
15. Cox B, Emili A. Tissue subcellular fractionation and protein extraction for use in mass-spectrometry-based proteomics. Nature Protocols. Nature Publishing Group; 2006;1:1872–8.
16. Bagni C, Klann E. Molecular functions of the mammalian fragile X mental retardation protein: insights into mental retardation and synaptic plasticity. The autisms: Molecules to model systems. 2012;126–46.
17. Maurin T, Bardoni B. Fragile X Mental Retardation Protein: To Be or Not to Be a Translational Enhancer. Frontiers in Molecular Biosciences. 2018;5:113.
18. Darnell JC, Van Driesche SJ, Zhang C, Hung KYS, Mele A, Fraser CE, et al. FMRP Stalls Ribosomal Translocation on mRNAs Linked to Synaptic Function and Autism. Cell. 2011;146:247–61.
19. Lombroso PJ. Genetics of childhood disorders: XLVIII. Learning and memory, Part 1: Fragile X syndrome update. Journal of the American Academy of Child and Adolescent Psychiatry. 2003;42:372–5.
20. Bear MF, Huber KM, Warren ST. The mGluR theory of fragile X mental retardation. Trends in Neurosciences. 2004;27:370–7.
21. Sullivan PF, Fan C, Perou CM. Evaluating the comparability of gene expression in blood and brain. American Journal of Medical Genetics Part B: Neuropsychiatric Genetics. 2006;141B:261–8.
22. Dieterich DC, Lee JJ, Link AJ, Graumann J, Tirrell DA, Schuman EM. Labeling, detection and identification of newly synthesized proteomes with bioorthogonal non-canonical amino-acid tagging. Nature Protocols. 2007;2:532–40.

23. Cox J, Mann M. MaxQuant enables high peptide identification rates, individualized p.p.b.-range mass accuracies and proteome-wide protein quantification. Nat Biotechnol. 2008;26:1367–72.
24. Cox J, Hein MY, Luber CA, Paron I, Nagaraj N, Mann M. Accurate Proteome-wide Label-free Quantification by Delayed Normalization and Maximal Peptide Ratio Extraction, Termed MaxLFQ. Mol Cell Proteomics. 2014;13:2513–26.
25. Tyanova S, Temu T, Sinitcyn P, Carlson A, Hein MY, Geiger T, et al. The Perseus computational platform for comprehensive analysis of (prote)omics data. Nature Methods. 2016;13:731–40.
26. Fabregat A, Jupe S, Matthews L, Sidiropoulos K, Gillespie M, Garapati P, et al. The Reactome Pathway Knowledgebase. Nucleic Acids Res. 2018;46:D649–55.
27. The Gene Ontology Resource: 20 years and still GOing strong. Nucleic Acids Res. 2019;47:D330–8.
28. Mi H, Muruganujan A, Huang X, Ebert D, Mills C, Guo X, et al. Protocol Update for large-scale genome and gene function analysis with the PANTHER classification system (v.14.0). Nature Protocols. 2019;14:703–21.
29. Handen A, Ganapthiraju MK. LENS: web-based lens for enrichment and network studies of human proteins. BMC Med Genomics. 2015;8:S2.
30. Ascano M, Mukherjee N, Bandaru P, Miller JB, Nusbaum JD, Corcoran DL, et al. FMRP targets distinct mRNA sequence elements to regulate protein expression. Nature. 2012;492:382–6.
31. Mayer G, Poirier S, Seidah NG. Annexin A2 is a C-terminal PCSK9-binding protein that regulates endogenous low density lipoprotein receptor levels. J Biol Chem. 2008;283:31791–801.
32. Ly K, Saavedra YG, Canuel M, Routhier S, Desjardins R, Hamelin J, et al. Annexin A2 reduces PCSK9 protein levels via a translational mechanism and interacts with the M1 and M2 domains of PCSK9. J Biol Chem. 2014;289:17732–46.
33. Seidah NG, Poirier S, Denis M, Parker R, Miao B, Mapelli C, et al. Annexin A2 is a natural extrahepatic inhibitor of the PCSK9-induced LDL receptor degradation. PLoS ONE. 2012;7:e41865.
34. Ben Djoudi Ouadda A, Gauthier M-S, Susan-Resiga D, Girard E, Essalmani R, Black M, et al. Ser-Phosphorylation of PCSK9 (Proprotein Convertase Subtilisin-Kexin 9) by Fam20C (Family With Sequence Similarity 20, Member C) Kinase Enhances Its Ability to Degrade the LDLR (Low-Density Lipoprotein Receptor). ATVB. 2019;39:1996–2013.
35. Jin J, Bhatti DL, Lee K-W, Medrihan L, Cheng J, Wei J, et al. Ahnak scaffolds p11/Anxa2 complex and L-type voltage-gated calcium channel and modulates depressive behavior. Mol Psychiatry. 2019;
36. Michalon A, Sidorov M, Ballard TM, Ozmen L, Spooren W, Wettstein JG, et al. Chronic Pharmacological mGlu5 Inhibition Corrects Fragile X in Adult Mice. Neuron. 2012;74:49–56.
37. Weng N, Weiler IJ, Sumis A, Berry-Kravis E, Greenough WT. Early-phase ERK activation as a biomarker for metabolic status in fragile X syndrome. American Journal of Medical Genetics Part B: Neuropsychiatric Genetics. 2008;147B:1253–7.
38. Bhattacharya A, Kaphzan H, Alvarez-Dieppa AC, Murphy JP, Pierre P, Klann E. Genetic Removal of p70 S6 Kinase 1 Corrects Molecular, Synaptic, and Behavioral Phenotypes in Fragile X Syndrome Mice.

Neuron. 2012;76:325–37.

39. Wang X, Snape M, Klann E, Stone JG, Singh A, Petersen RB, et al. Activation of the extracellular signal-regulated kinase pathway contributes to the behavioral deficit of fragile x-syndrome. Journal of Neurochemistry. 2012;121:672–9.
40. Shen L, Feng C, Zhang K, Chen Y, Gao Y, Ke J, et al. Proteomics Study of Peripheral Blood Mononuclear Cells (PBMCs) in Autistic Children. Frontiers in Cellular Neuroscience. 2019;13:105.
41. Legate KR, Montañez E, Kudlacek O, Füssler R. ILK, PINCH and parvin: the tIPP of integrin signalling. Nature Reviews Molecular Cell Biology. 2006;7:20–31.
42. Lai-Cheong JE, Parsons M, McGrath JA. The role of kindlins in cell biology and relevance to human disease. The International Journal of Biochemistry & Cell Biology. 2010;42:595–603.
43. Legate KR, Wickström SA, Fässler R. Genetic and cell biological analysis of integrin outside-in signaling. Genes Dev. 2009;23:397–418.
44. Walker JL, Fournier AK, Assoian RK. Regulation of growth factor signaling and cell cycle progression by cell adhesion and adhesion-dependent changes in cellular tension. Cytokine & Growth Factor Reviews. 2005;16:395–405.
45. Chen H-C, Appeddu PA, Isoda H, Guan J-L. Phosphorylation of Tyrosine 397 in Focal Adhesion Kinase Is Required for Binding Phosphatidylinositol 3-Kinase. J Biol Chem. 1996;271:26329–34.
46. Webb DJ, Donais K, Whitmore LA, Thomas SM, Turner CE, Parsons JT, et al. FAK–Src signalling through paxillin, ERK and MLCK regulates adhesion disassembly. Nat Cell Biol. 2004;6:154–61.
47. Pankov R, Cukierman E, Clark K, Matsumoto K, Hahn C, Poulin B, et al. Specific beta1 integrin site selectively regulates Akt/protein kinase B signaling via local activation of protein phosphatase 2A. J Biol Chem. 2003;278:18671–81.
48. Ivaska J, Nissinen L, Immonen N, Eriksson JE, Kähäri V-M, Heino J. Integrin alpha 2 beta 1 promotes activation of protein phosphatase 2A and dephosphorylation of Akt and glycogen synthase kinase 3 beta. Mol Cell Biol. 2002;22:1352–9.
49. Kumari D, Bhattacharya A, Nadel J, Moulton K, Zeak NM, Glicksman A, et al. Identification of Fragile X Syndrome Specific Molecular Markers in Human Fibroblasts: A Useful Model to Test the Efficacy of Therapeutic Drugs. Human Mutation. 2014;35:1485–94.
50. Gross C, Bassell GJ. Excess Protein Synthesis in FXS Patient Lymphoblastoid Cells Can Be Rescued with a p110β-Selective Inhibitor. Molecular Medicine. 2012;18:336–45.
51. Gross C, Nakamoto M, Yao X, Chan C-B, Yim SY, Ye K, et al. Excess Phosphoinositide 3-Kinase Subunit Synthesis and Activity as a Novel Therapeutic Target in Fragile X Syndrome. Journal of Neuroscience. 2010;30:10624–38.
52. McGeachie AB, Cingolani LA, Goda Y. A stabilising influence: Integrins in regulation of synaptic plasticity. Neurosci Res. 2011;70:24–9.
53. Park YK, Goda Y. Integrins in synapse regulation. Nat Rev Neurosci. 2016;17:745–56.

54. Ferrer-Ferrer M, Dityatev A. Shaping Synapses by the Neural Extracellular Matrix. Front Neuroanat [Internet]. 2018 [cited 2019 Dec 16];12. Available from: https://www.ncbi.nlm.nih.gov/pmc/articles/PMC5962695/
55. Cingolani LA, Thalhammer A, Yu LMY, Catalano M, Ramos T, Colicos MA, et al. Activity-dependent regulation of synaptic AMPA receptor composition and abundance by beta3 integrins. Neuron. 2008;58:749–62.
56. Shi Y, Ethell IM. Integrins control dendritic spine plasticity in hippocampal neurons through NMDA receptor and Ca2+/calmodulin-dependent protein kinase II-mediated actin reorganization. J Neurosci. 2006;26:1813–22.
57. Chan C-S, Weeber EJ, Zong L, Fuchs E, Sweatt JD, Davis RL. β1-Integrins Are Required for Hippocampal AMPA Receptor-Dependent Synaptic Transmission, Synaptic Plasticity, and Working Memory. J Neurosci. 2006;26:223–32.
58. Sidhu H, Dansie LE, Hickmott PW, Ethell DW, Ethell IM. Genetic Removal of Matrix Metalloproteinase 9 Rescues the Symptoms of Fragile X Syndrome in a Mouse Model. J Neurosci. 2014;34:9867–79.
59. Janusz A, Milek J, Perycz M, Pacini L, Bagni C, Kaczmarek L, et al. The Fragile X Mental Retardation Protein Regulates Matrix Metalloproteinase 9 mRNA at Synapses. Journal of Neuroscience. 2013;33:18234–41.
60. Bilousova TV, Dansie L, Ngo M, Aye J, Charles JR, Ethell DW, et al. Minocycline promotes dendritic spine maturation and improves behavioural performance in the fragile X mouse model. J Med Genet. 2009;46:94–102.
61. Gkogkas CG, Khoutorsky A, Cao R, Jafarnejad SM, Prager-Khoutorsky M, Giannakas N, et al. Pharmacogenetic Inhibition of eIF4E-Dependent Mmp9 mRNA Translation Reverses Fragile X Syndrome-like Phenotypes. Cell Reports. 2014;9:1742–55.
62. Sidorov MS, Auerbach BD, Bear MF. Fragile X mental retardation protein and synaptic plasticity. Molecular Brain. 2013;6:15.
63. Shang Y, Wang H, Mercaldo V, Li X, Chen T, Zhuo M. Fragile X mental retardation protein is required for chemically-induced long-term potentiation of the hippocampus in adult mice. J Neurochem. 2009;111:635–46.
64. Bostrom CA, Majaess N-M, Morch K, White E, Eadie BD, Christie BR. Rescue of NMDAR-Dependent Synaptic Plasticity in Fmr1 Knock-Out Mice. Cereb Cortex. 2015;25:271–9.
65. Suvrathan A, Hoeffer CA, Wong H, Klann E, Chattarji S. Characterization and reversal of synaptic defects in the amygdala in a mouse model of fragile X syndrome. Proc Natl Acad Sci U S A. 2010;107:11591–6.
66. Hynes RO. Integrins: Bidirectional, Allosteric Signaling Machines. Cell. 2002;110:673–87.
67. Pellerin D, Lortie A, Corbin F. Platelets as a surrogate disease model of neurodevelopmental disorders: Insights from Fragile X Syndrome. Platelets. 2018;29:113–24.
68. Boisvert F-M, Ahmad Y, Gierliński M, Charrière F, Lamont D, Scott M, et al. A Quantitative Spatial Proteomics Analysis of Proteome Turnover in Human Cells. Molecular & Cellular Proteomics.

2012;11:M111.011429.

69. Bian F, Simon RP, Li Y, David L, Wainwright J, Hall CL, et al. Nascent Proteomes in Peripheral Blood Mononuclear Cells as a Novel Source for Biomarker Discovery in Human Stroke. Stroke. 2014;45:1177–9.

# Figures

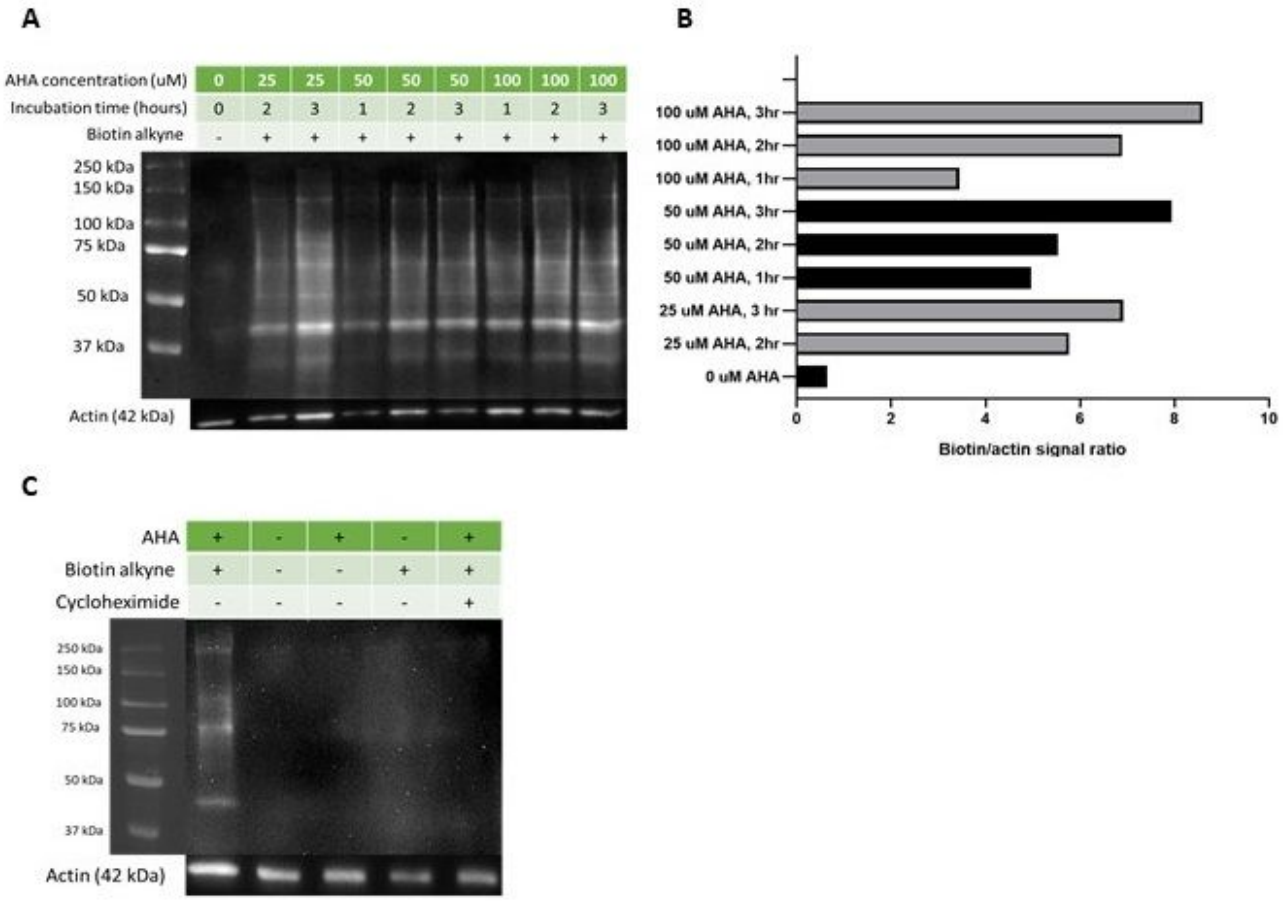


Figure 1

**Figure 1**

Determination of the optimal AHA labelling condition A) Anti-biotin Western Blot of proteins extracts obtained from PBMCs under different AHA labelling conditions. B) Quantification of the biotin signal obtained by Western blot. Biotin signal intensities were normalised with the corresponding actin signal. C) Specificity of the AHA labelling and conjugation of the biotin probe towards newly synthetize proteins.

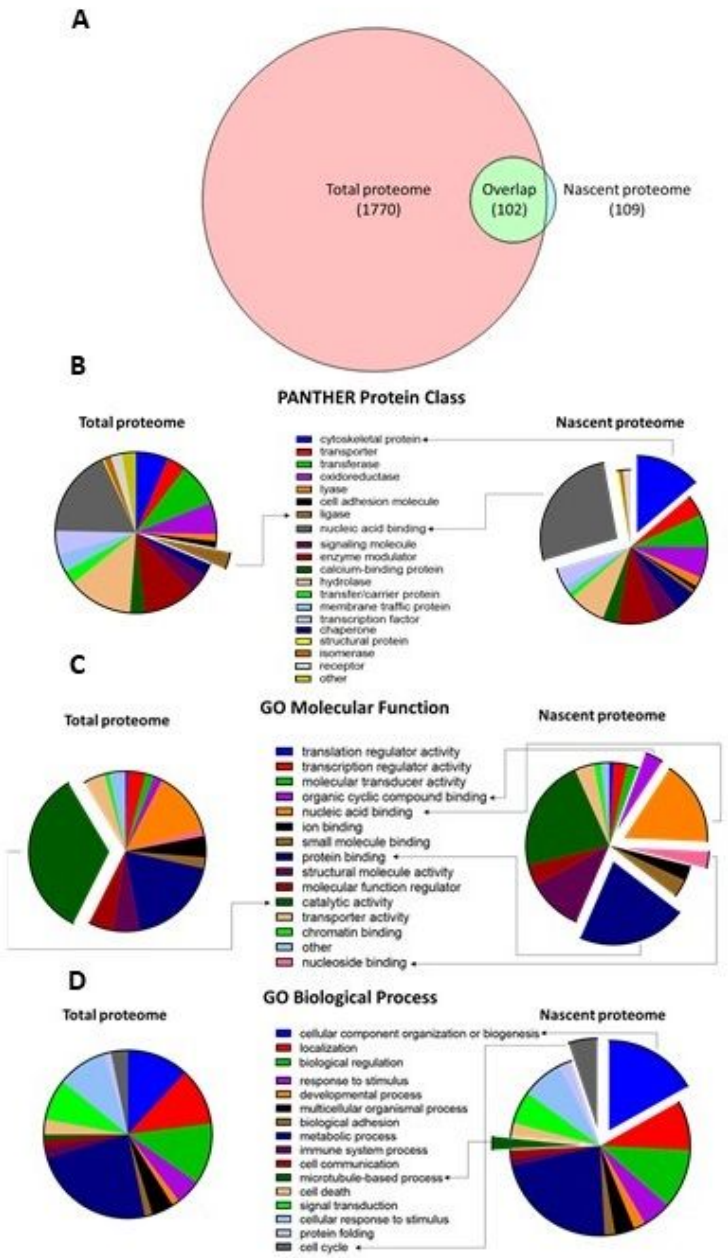


Figure 2

## Figure 2

Comparison between the nascent and total proteome. The nascent proteome is less complex then the total proteome. A) Venn diagrams representing the number of proteins identified in the proteomic screening. The nascent proteome is enriched in proteins associated with specific Gene Ontology terms. A fisher exact test was used to determine enriched annotations between the two proteomes. An FDR inferior to 0.05 was considered significative. Pie chart representing the distribution of different annotations

between the two proteomes: PANTHER protein class (B), Gene Ontology molecular function (C) and biological process (D). The exposed part represents enriched annotations in the corresponding proteome.

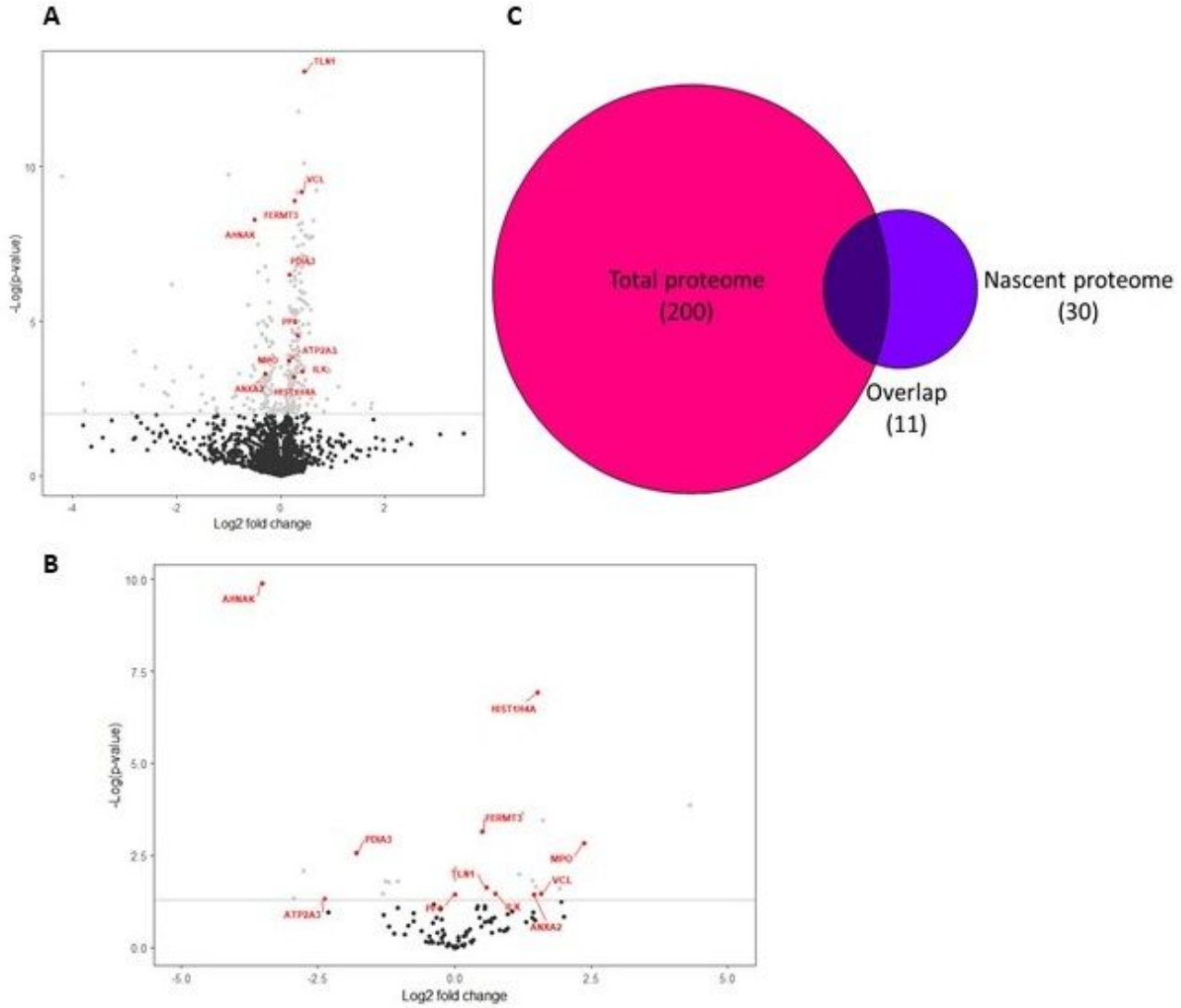


Figure 3

## Figure 3

Differentially expressed proteins are found in fragile X PBMCs. A) Volcano plot of the proteins identified in the total proteome of PBMCs. The horizontal bar represents a p-value of 0.01, which was considered significative. B) Volcano plot of the proteins identified in the nascent proteome of PBMCs. The horizontal bar represents a p-value of 0.05, which was considered significative. The proteins marked in red are found to be differentially expressed in both proteomes. C) Venn diagram of the number of differentially expressed proteins found in both fragile X nascent and total proteome.

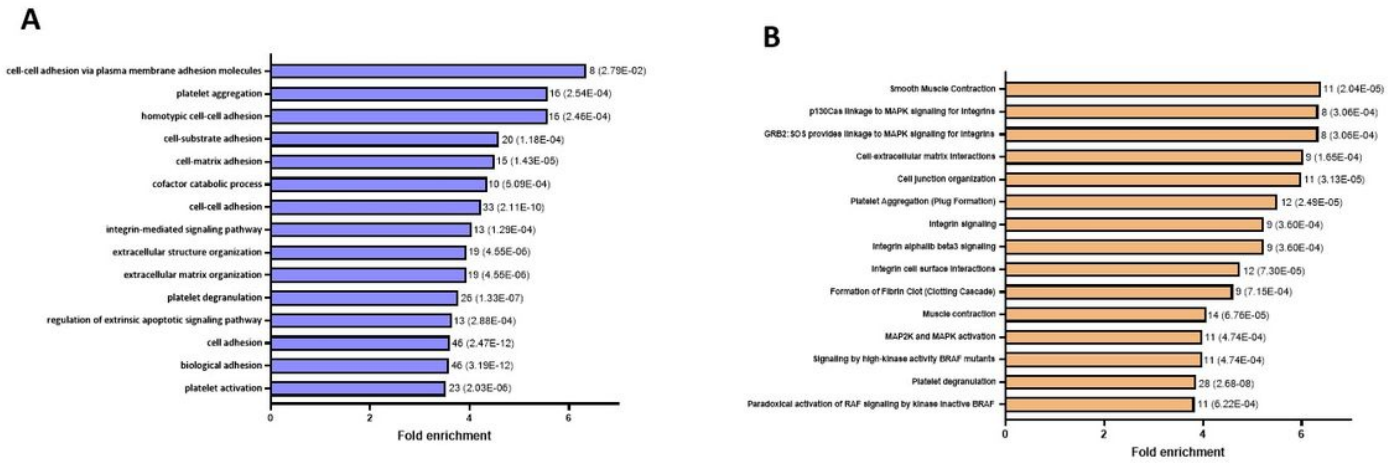


Figure 4

## Figure 4

Functional annotation enrichment analysis of the differentially expressed proteins found in fragile X PBMCs total proteome. The number of proteins associated and corresponding FDR for each annotation are represented beside the bar. A) The top 15 gene ontology biological process annotations ranked by the fold enrichment. B) The top 15 REACTOME annotations ranked by the fold enrichment.

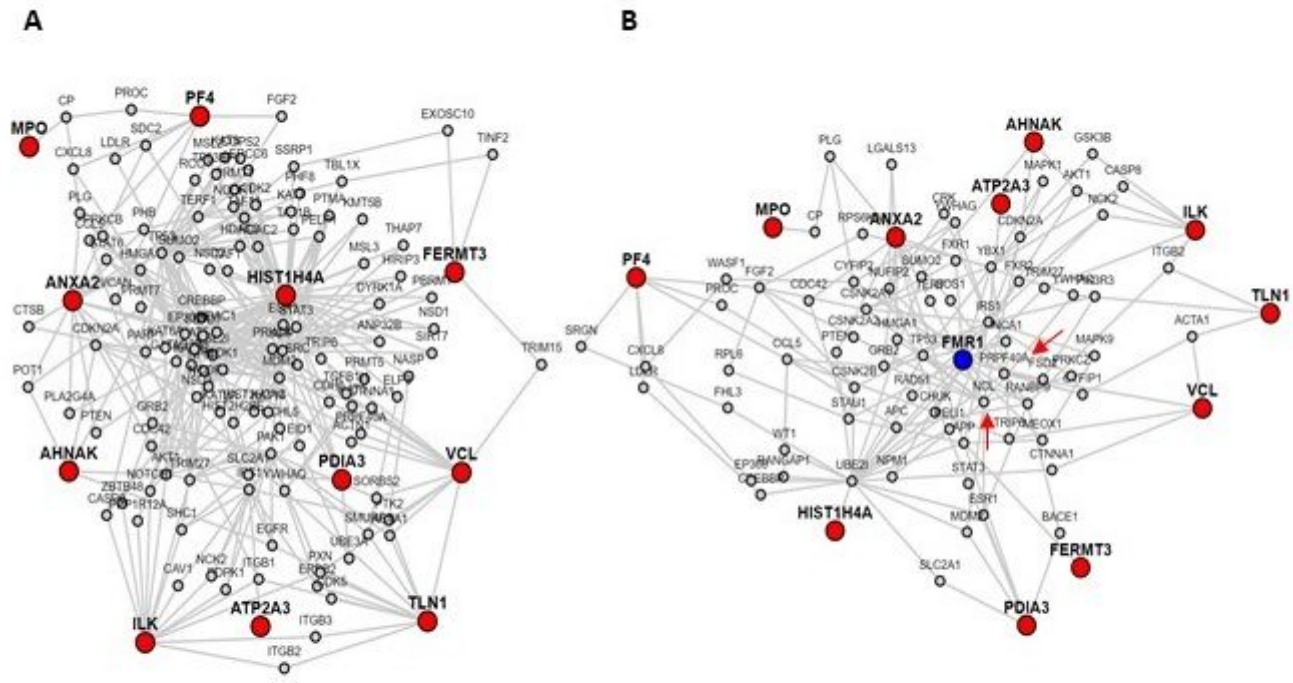


Figure 5

**Figure 5**

Protein-protein interaction network of 11 proteins found differentially expressed in both nascent and total proteome of fragile X PBMCs. A) Interaction network corresponding only of the 11 candidates (red). B) Interaction network generated with the 11 candidate proteins (red) and FMRP (blue) set as target. The NCL and PRPF40A proteins, which are found dysregulated in FXS nascent proteome, are also present in this network (red arrows).

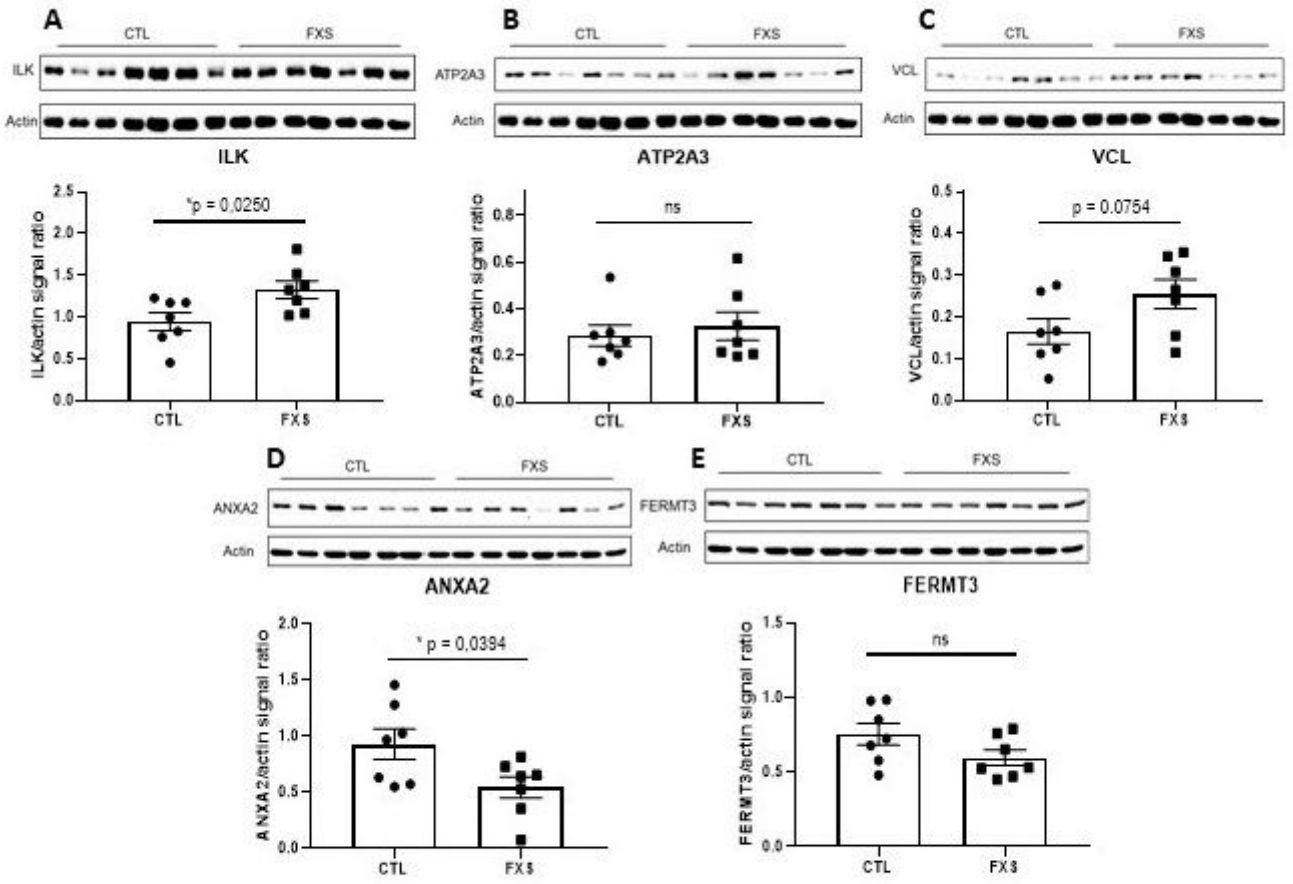


Figure 6

**Figure 6**

Validation of 5 candidate proteins by Western Blot. A) Integrin-linked protein kinase (ILK) B) Sarcoplasmic/endoplasmic reticulum calcium ATPase 3 (ATP2A3) C) Vinculin (VCL) D) Annexin A2 (ANXA2) E) Fermitin family homolog 3 (FERMT3) F). Signal of all proteins were normalised to the actin signal to account for loading disparity. A two-tailed student t-test was used to calculate the significance of the difference measured between the two groups.

# Supplementary Files

This is a list of supplementary files associated with this preprint. Click to download.

- TableS1DionneetCorbin2021BiomarkerResearch.xlsx
- TableS2DionneetCorbin2021BiomarkerResearch.xlsx
- TableS3DionneetCorbin2021BiomarkerResearch.xlsx
- TableS4DionneetCorbin2021BiomarkerResearch.xlsx